Journal of Structural Engineering & Applied Mechanics (2023) 6(2):117-128
DOI 10.31462/jseam.2023.02117128

RESEARCH ARTICLE

Effects of beam-column connection rigidities and soil-structure interaction on seismic performance of steel frames

Meryem Karakurt[1], Korhan Özgan[2*]

[1] Ilbank Trabzon Regional Directorates, Trabzon, Türkiye
[2] Karadeniz Technical University, Department of Civil Engineering, Trabzon, Türkiye

Article History

Received 11 May 2023
Accepted 13 June 2023

Keywords

Pushover analysis
Steel frame
Pasternak model
Seismic performance

Abstract

Structures can be exposed to non-linear deformations under earthquake effects. However, linear methods are mostly preferred for designs because of their simplicity and facility. The inelastic behavior of the structure is approximately taken into account by using some coefficients. However, it is possible to make more realistic and economical designs by using methods that consider the inelastic behavior of the structure. In this context, the displacement-based design method is becoming increasingly popular. This study evaluates the seismic performance of steel frames resting on elastic foundations with different beam-column joint stiffnesses using the static pushover analysis method. Static pushover curves, plastic deformations, performance points, and base shear forces were compared. The results show that the base condition greatly affects the seismic performance of the building.

1. Introduction

Recent earthquakes have demonstrated that structural damage can lead to significant economic losses and loss of life. The damages especially in beam-column joints cause the structures to fail to show the expected strength during earthquakes and to collapse partially or completely. Consequently, the behavior of buildings under seismic activity is a critical area of study in civil engineering. To address this issue, national seismic codes are periodically updated to incorporate modern design approaches that can improve structural integrity during earthquakes [1]. There is growing interest in deformation-based design methods, which allow for more realistic assessments of a structure's seismic performance by taking into account its non-linear behavior. Unlike the force-based design method, which assumes linear behavior, the deformation-based approach enables engineers to design structures that meet desired performance levels. This method is particularly useful for assessing the seismic performance of existing structures and identifying elements or sections that require strengthening. As a result, it is a more effective approach to designing earthquake-resistant structures.

Previous studies on performance-based nonlinear design are summarized below. Krawinkler and Seneviranta [2] published a study in 1998 that outlined the basic principles of non-linear static pushover analysis. Static pushover analysis was used by Chopra and Goel [3] to determine the seismic demands due to increased earthquake loads, using the distribution of inertia forces for each mode. To assess the sensitivity of non-linear static pushover analyses, Chintanapakdee and Chopra [4] conducted experiments using 3, 6, 9,

* Corresponding author (kozgan@ktu.edu.tr)
eISSN 2630-5763

12, 15, and 18-story frames. Bayülke, Kuran, and Kocaman [5] applied static pushover analysis to earthquake-damaged and reinforced structures, comparing the damages and lateral load-bearing capacities of the structures and discussing the causes of damage. Edgar and Sorto [6] performed displacement-controlled pushover analyses on two types of towers to determine the order of failure and safety level, modeling structural elements using beam and column elements with lumped plastic hinges in SAP2000 software. Moghaddam and Hajirasouliha [7] investigated the potential of pushover analysis to estimate the seismic deformation demands of concentrically braced steel frames. Kaley and Baig [8] used SAP2000 software to study pushover analysis of a typical multi-story steel frame building with and without various types of bracings. Kalibhat et al. [9] investigated the effect of concentric bracings on the seismic performance of steel frames. Mirjalili and Rofooei [10] proposed a modified dynamic-based pushover analysis that properly considers the effects of higher modes and the nonlinear behavior of structural systems.

The study aims to examine the effects of beam-column connection rigidities on the seismic behavior of steel frames, considering the soil-structure interaction. For this purpose, a three-span steel frame with a span of 5 meters has been chosen for numerical applications. Three different beam-column connection types are considered: rigid, semi-rigid, and pinned. Frame models with 4, 6, and 8 floors are examined separately. Soil-structure interaction is taken into account using the Pasternak model. Static pushover analyses are performed on the frames using SAP2000 commercial software [11].

2. Non-linear static pushover analysis

The nonlinear static pushover analysis method is employed to determine and evaluate the performance of structures under earthquake ground motion. In the method, the force-displacement relationship of the structure is considered according to the nonlinear theory in terms of materials and geometry. As a result, it enables designers to identify unsafe structural members and assess whether the structures can withstand seismic loads and perform as expected.

To evaluate the performance of the structure, pushover analysis is performed under vertical loads by increasing horizontal loads, and the capacity curve of the structure is obtained. The capacity curve is a graph showing the peak displacement values corresponding to the base shear forces. However, to compare the capacity curve with the demand curve, it is converted to a modal capacity curve. The spectral acceleration and spectral displacement axes in the modal capacity curve are calculated using the following equations.

$$PF_1 = \frac{\sum_{i=1}^{N} m_i \emptyset_{i1}}{\sum_{i=1}^{N} m_i \emptyset_{i1}^2} \tag{1}$$

$$\alpha_1 = \frac{\left[\sum_{i=1}^{N} m_i \emptyset_i\right]^2}{\left[\sum_{i=1}^{N} m_i\right]\left[\sum_{i=1}^{N} m_i \emptyset_{i1}^2\right]} \tag{2}$$

$$S_a = \frac{V/W}{\alpha_1} \tag{3}$$

$$S_d = \frac{\Delta_{roof}}{PF_1 \emptyset_{roof,1}} \tag{4}$$

where

PF_1	= modal participation factor for the first natural mode
α_1	= modal mass coefficient for the first natural mode
m_i	= mass assigned to level i
$\emptyset_{i1}$	= amplitude of mode 1 at level i
N	= level N, the level which is the uppermost in the main portion of the structure

V	= base shear
W	= building dead weight plus likely live load
Δ_{roof}	= roof displacement
S_a	= spectral acceleration
S_d	= spectral displacement

In the second step, the demand curve consisting of the spectral acceleration (S_a) and period (T) values of the structure are drawn (Fig. 1).

C_A and C_V show peak acceleration coefficient of the ground and 5% damped response of a 1-second system. C_A and C_V parameters depend on the earthquake zone and earthquake source distance. These parameters are determined depending on the earthquake zone coefficient Z, the earthquake effect type coefficient E, the coefficient N of the distance to the earthquake source, and the soil class. These coefficients are taken from the tables given in the ATC-40.

To compare the elastic demand spectrum curve with the modal capacity curve, the period (T) values on the horizontal axis must be converted to spectral displacement (S_d) values. Equation (5) is used for this conversion.

$$S_d(T) = \frac{T^2}{4\pi^2} S_a g \tag{5}$$

In the third step, the required performance point is calculated by intersecting the capacity and demand curves on the same graph (Fig. 2). After conducting a pushover analysis, the seismic performance of the building is evaluated by examining the plastic deformations in its structural members. The plastic deformation limits for these members are provided in ATC-40 [12] and FEMA356 [13].

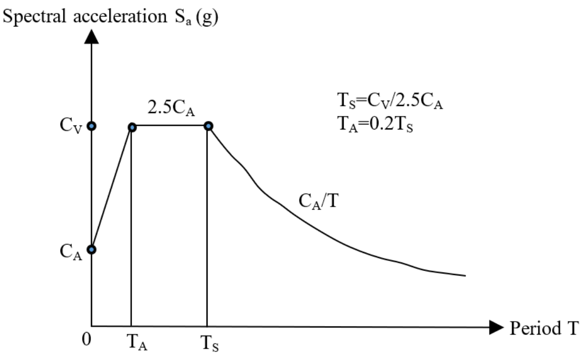

Fig. 1. Elastic acceleration spectrum curve according to ATC-40 [12]

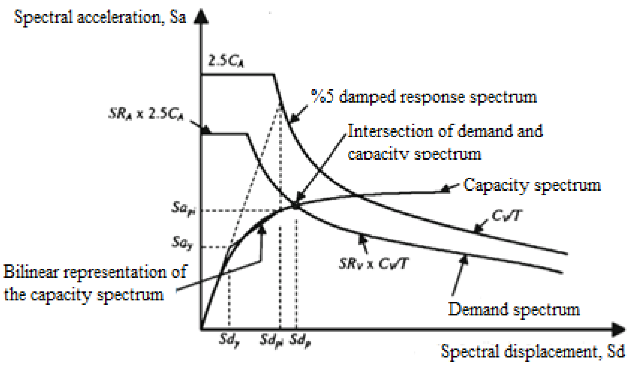

Fig. 2. Demand and capacity spectrum curves [12]

3. Pasternak model

The soil properties of the building significantly affect the behavior of the building. Loads transferred from the building cause deformations in the subsoil and the reaction of the subsoil changes the internal forces in the building. One of the models that consider the subsoil effects on the building is the model developed by Pasternak, which provides continuity in the subsoil by taking shear effects into the soil account. In the model, subsoil reactions are represented with the following expression.

$$q(x) = Cw(x) - 2C_t(\partial^2 w/\partial x^2) \tag{6}$$

Here q, C, w and C_t denote subsoil reaction, subgrade reaction modulus, vertical displacement, and shear coefficient respectively. Subsoil parameters are as follows:

$$C = \frac{E_s}{H(1+\nu_s)(1-2\nu_s)} \tag{7}$$

$$C_t = \frac{E_s H}{6(1+\nu_s)} \tag{8}$$

where E_s is the elasticity modulus of the subsoil, ν_s is the Poisson ratio and H is subsoil depth. In this study, analyses were carried out with SAP2000v21.2.0 [11] commercial software. SAP2000 is capable of modeling the building with the Winkler subsoil model using linear springs. The approach developed by Tahaoğlu [14] was used to represent the Pasternak subsoil model, considering the interaction between the springs with the shear parameter. In this approach, soil elements are defined under the building. Tahaoğlu [14] neglected the bending stiffness of the soil elements by multiplying it with a very small value close to zero. It also increased the axial stiffness by multiplying it by a very large number and prevented out-of-plane deformations.

4. Findings and discussion

A three-span steel frame consisting of four, six, and eight stories was chosen for numerical analysis. The floor heights are 3 meters and the beam spans are five meters. The steel grade used is S275. The beam-column connections were considered rigid, semi-rigid, and pinned separately. The beams were subjected to 7.5 kN/m dead load and 5.0 kN/m live load in addition to the self-weight of the frame. The demand curve was obtained according to the ATC-40 [12] code. The earthquake zone coefficient is taken as $Z = 0.4$ and, the soil class as SD. $E = 1.0$ was chosen so that the earthquake effect type coefficient could correspond to the design earthquake. The distance to the earthquake source is five km. C_A and C_V coefficients are determined as 0.528 and 1.024, respectively The horizontal earthquake load for each floor is calculated using modal analysis, proportional to the floor displacements and weights, and is applied to the floor levels. A view of the 4-story frame is given in Fig. 3.

A lumped plastic hinge approach was used to consider the non-linear behavior of the frame. In columns, two hinges (P-M3) were defined at the column ends. In the beams, three hinges (M3) were defined at the beam ends and the middle of the span. Second-order effects ($P - \Delta$) were also taken into account in the analysis. The stiffness value calculated for the semi-rigid connection type is given below.

$$k = \frac{4EI}{L} = \frac{4 \times 2.1 \times 10^8 \times 1.777 \times 10^{-4}}{5} = 29853.6 \text{ kNm}$$

$$n \times (1-n) \times k = 0.5 \times (1-0.5) \times 29853.6 = 7463.4 \text{ kNm}$$

The moment-curvature graphic in Fig. 4 illustrates the performance level limits.

Fig. 3. 4-story plane steel frame model

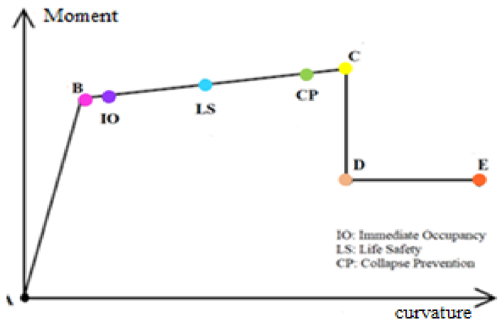

Fig. 4. Damage status ranges on the capacity curve

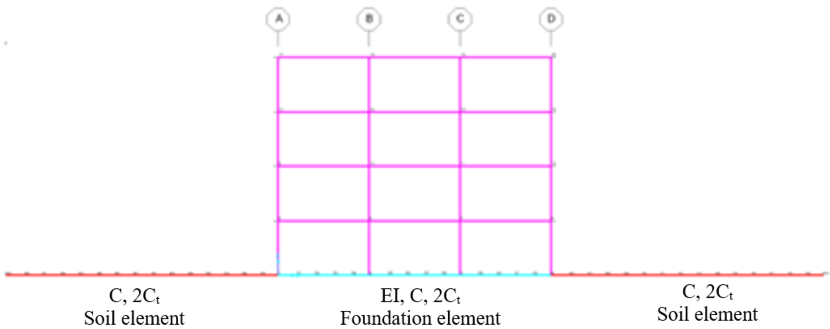

Fig. 5. Analysis model of a 4-story steel frame considering soil-structure interaction

Footing and subsoil were modeled with a beam element of 0.5×0.5 m. Beam elements were divided into finite elements of 1 meter. The modulus of elasticity for the concrete is taken as $E = 33000$ MPa. An analysis model of a 4-story steel frame on a Pasternak-type elastic foundation is shown in Fig. 5. The subgrade reaction modulus and shear parameter of the subsoil are as follows: for hard soil, $C = 3000\ \mathrm{kN/m^2}$ and $2C_t = 1000$ kN; for medium hard soil, $C = 1500\ \mathrm{kN/m^2}$ and $2C_t = 2000$ kN; for soft soil, $C = 750\ \mathrm{kN/m^2}$ and $2C_t = 3000$ kN.

For the 4-story frame, the target displacement of 0.96 m was determined, which corresponds to 8% of the building height. Pushover analysis was performed, and the base shear forces corresponding to a 0.96 m horizontal displacement at the roof of the frame are presented in Fig. 6. As seen, the horizontal rigidity of the frame decreases as the stiffness of the beam-column connection decreases, leading to a decrease in the base shear force. Larger base shear force values were obtained for all connection types when the subsoil model was considered.

The sections where plastic rotations occur and the corresponding plastic rotation levels are illustrated in Fig. 7 when the target displacement was reached. According to Fig. 6, when the soil softens, the base shear force approaches the solutions obtained without considering the elastic soil. Fig. 7 explains this unexpected result. It shows that the frame fixed at the base has already reached the collapse level and is therefore exposed to less base shear force. In other words, the flexibility due to subsoil prevents the increase in plastic rotations in the column-foundation joint in other models. This is the opposite of the natural vibration periods of the frames. As the subsoil stiffens, the periods get closer to the periods of the frame with a fixed base, as expected. Furthermore, it can be seen that the number of hinges decreases for soft subsoil conditions. The plastic rotations remain between the immediate occupancy (IO) and life safety (LS) levels for all subsoil types. Particularly, it can be seen that the column sections at the collapse level for the fixed base frame are on the safe side considering the soil-structure interaction.

As seen in Table 2, as the soil softens, base shear forces decrease while horizontal displacements increase. Moreover, as the beam-column connection stiffnesses decrease, the horizontal displacement increases, and the base shear forces decrease.

The target displacement of the 6-story frame was determined as 1.44 m taking 8% of the building height and pushover analysis was performed. The base shear forces corresponding to 1.44 m horizontal displacement at the roof of the frame are presented in Fig. 8. As seen, the trend of the results for the frames with soil-structure interaction is similar to that for the rigid-base assumption. For all support conditions, it is seen that as the beam-column connection stiffness decreases, the horizontal stiffness of the structure decreases and accordingly the base shear force decreases. Larger base shear forces were observed in the frames resting on elastic foundations.

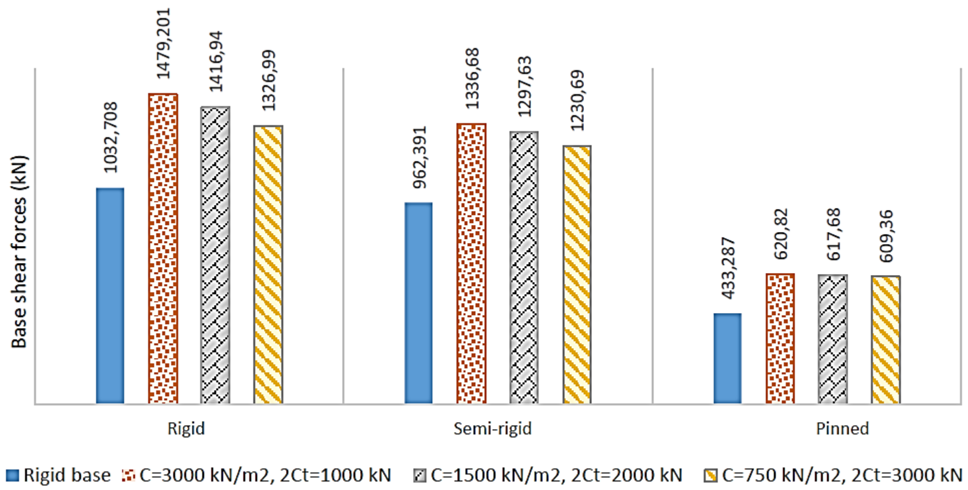

Fig. 6. Base shear forces depending on the support condition for a 4-story steel frame

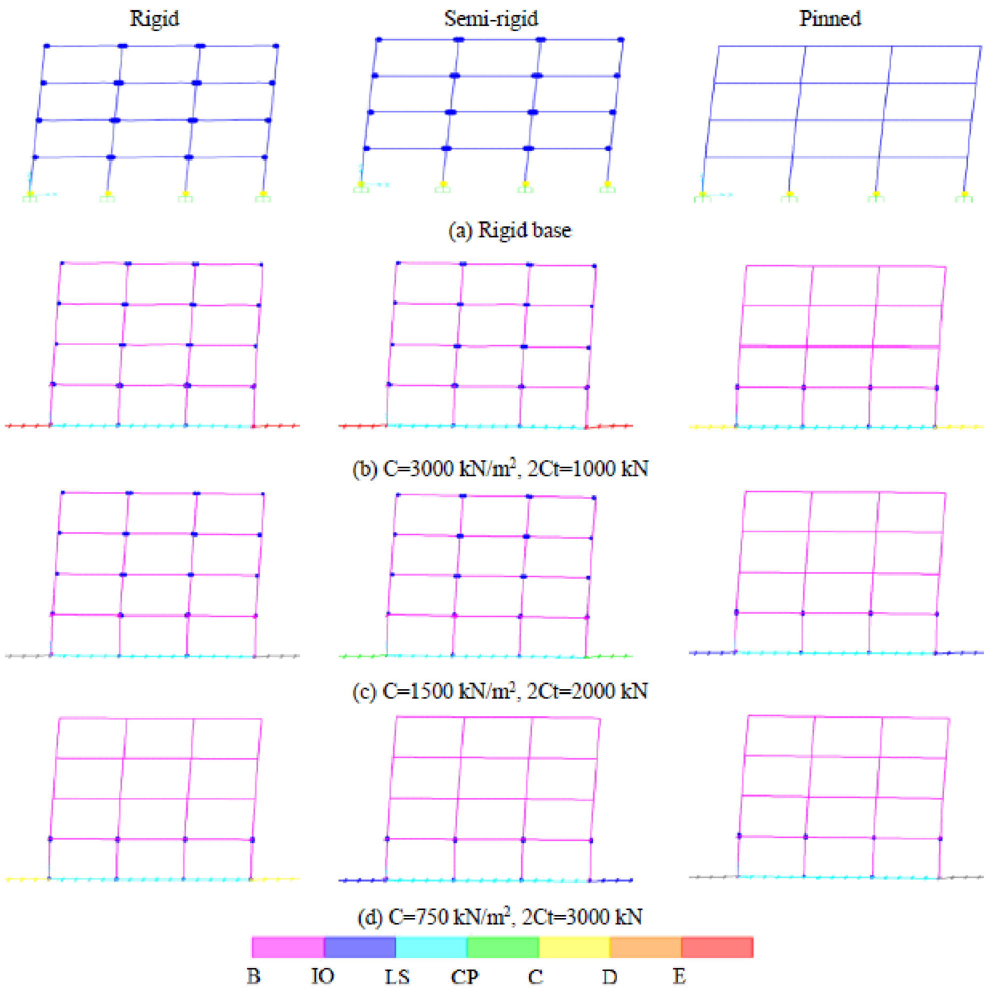

Fig. 7. Plastic hinges in a 4-story steel frame under target displacement

Table 2. Base shear forces and horizontal displacements on performance point for a 4-story steel frame

	Rigid base		Hard soil		Medium hard soil		Soft soil	
Connection type	V (kN)	u (m)	V (kN)	u (m)	V (kN)	u (m)	V (kN)	u (m)
Rigid	553.36	0.08	630.07	0.18	615.56	0.22	574.69	0.27
Semi-rigid	520.18	0.19	571.97	0.27	533.18	0.29	479.47	0.31
Pinned	381.70	0.35	374.35	0.38	363.30	0.39	346.14	0.41

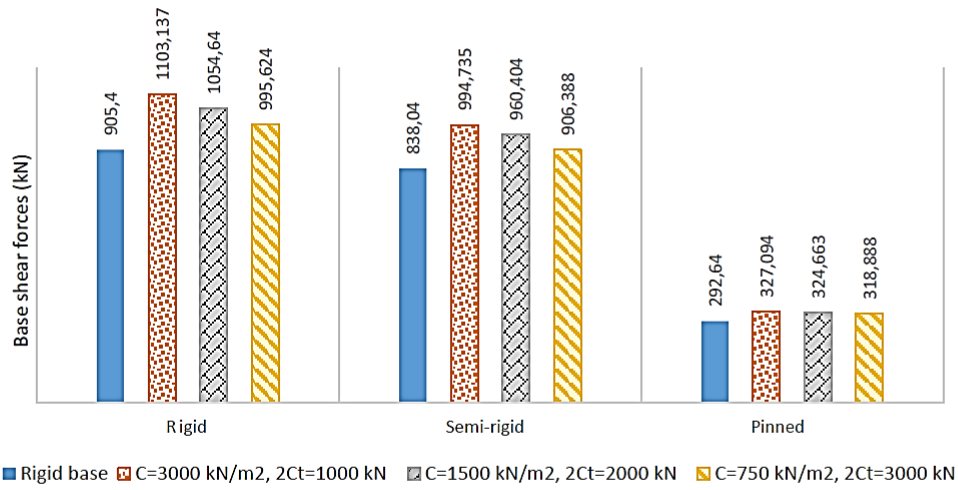

Fig. 8. Base shear forces depending on the support condition for a 6-story steel frame

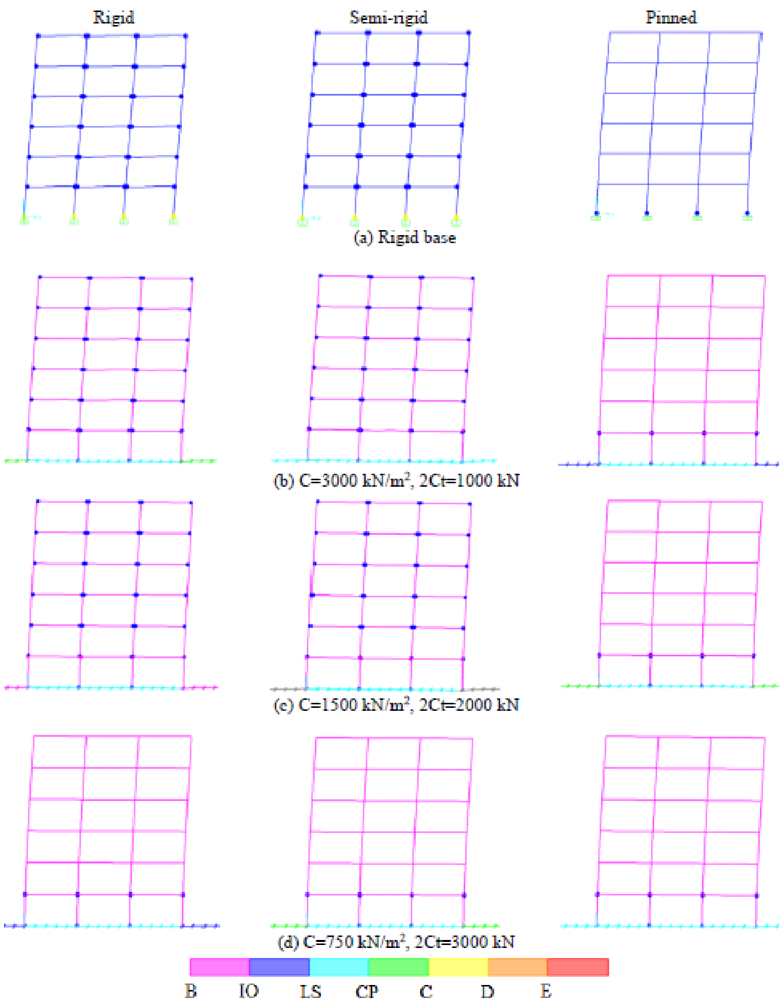

Fig. 9. Plastic hinges in a 6-story steel frame under target displacement

The number and level of hinges for the target displacement are given in Fig. 9. In the case of a rigid base, as well as for rigid and semi-rigid beam-column connections, it is observed that plastic rotations at the bottom of the first-story column exceed the collapse prevention level. In other words, the subsoil's flexibility prevents an increase in the plastic rotations at the column-foundation joint. Additionally, in the six-story models, it is clearer that the number of hinges and plastic rotations decreases as the stiffness of the subsoil decreases.

Performance points were obtained by comparing the capacity curves of each model with the earthquake demand curves, as shown in Table 3. As the rigidity of the subsoil decreases, the horizontal displacements of frames at the performance points increase, while the base forces decrease. Additionally, as the beam-column connection stiffnesses decrease, the horizontal displacement increases and the base shear forces decrease. As the subsoil hardens, the base shear force and horizontal displacement values are obtained by considering the soil-structure interaction approach and the results of the frame with the fixed base. Conversely, the first-floor columns of the frame with a fixed base reached the collapse level when the frames were pushed to the target displacement, resulting in the opposite situation.

The target displacement of the 8-story frame was determined as 1.92 m by taking 8% of the building height, and the model was subjected to a pushover analysis. The base shear force values are provided in Fig. 10. It is seen that the horizontal rigidity of the structure decreases, and accordingly, the base shear force decreases for all support conditions as the beam-column connection stiffness decreases. Larger base shear forces were obtained for the frames, taking soil-structure interaction into account. Table 4 shows base shear forces and horizontal displacements on performance point for the 8-story steel frame. The behavior is quite similar to that of the 4- and 6-story steel frames.

Table 3. Base shear forces and horizontal displacements on the performance point for a 6-story steel frame

	Rigid base		Hard soil		Medium hard soil		Soft soil	
Connection type	V (kN)	u (m)	V (kN)	u (m)	V (kN)	u (m)	V (kN)	u (m)
Rigid	643.26	0.20	623.44	0.33	566.14	0.39	482.82	0.47
Semi-rigid	543.07	0.38	488.63	0.46	448.53	0.50	395.85	0.56
Pinned	254.11	0.78	244.27	0.82	240.36	0.85	231.46	0.89

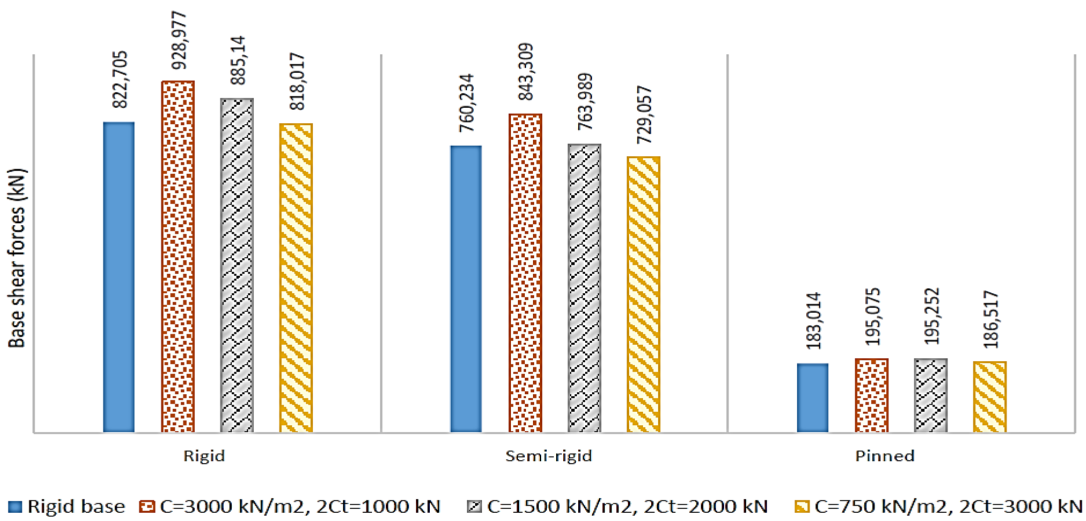

Fig. 10. Base shear forces depending on the support condition for an 8-story steel frame

Fig. 11 illustrates that plastic rotations in the bottom of the first story column for the frame with rigid and semi-rigid joints exceed the limit of collapse prevention. As a result, this frame is capable of bearing fewer base shear forces.

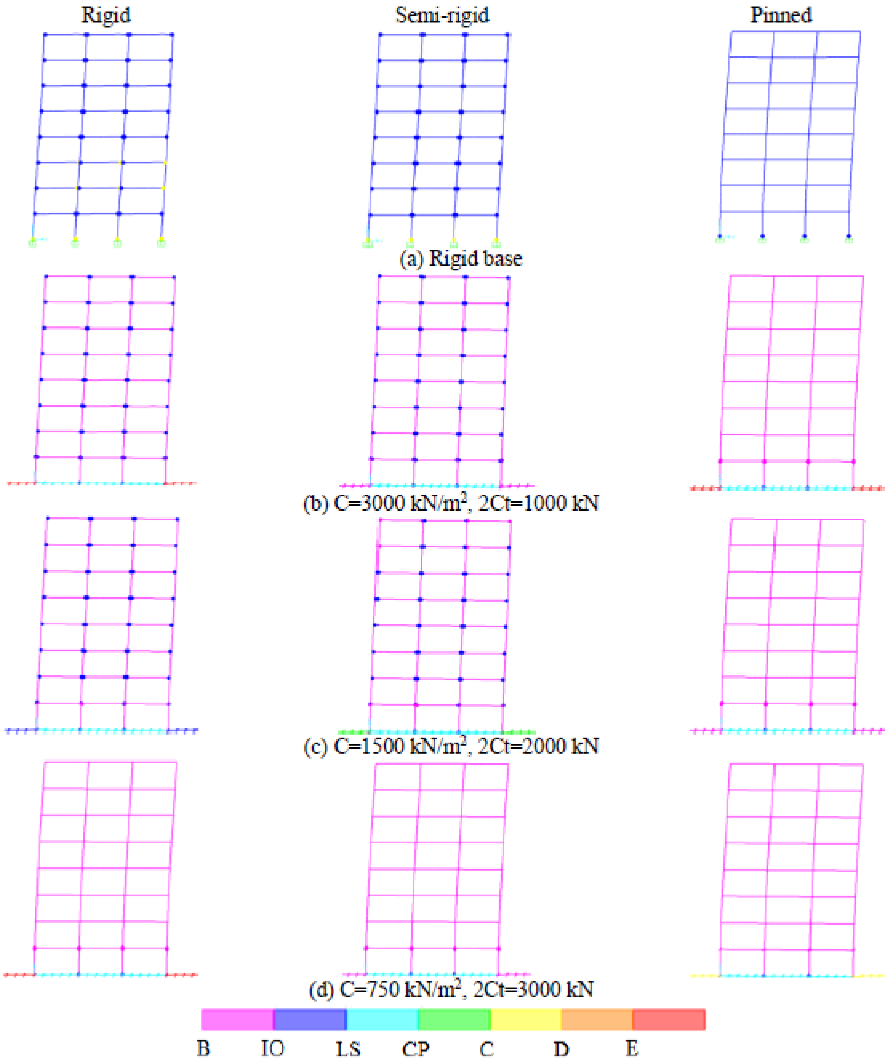

Fig. 11. Plastic hinges in an 8-story steel frame under target displacement

Table 4. Base shear forces and horizontal displacements on performance point for an 8-story steel frame

	Rigid base		Hard soil		Medium hard soil		Soft soil	
Connection type	V (kN)	u (m)	V (kN)	u (m)	V (kN)	u (m)	V (kN)	u (m)
Rigid	529.30	0.29	550.67	0.47	498.62	0.57	417.97	0.71
Semi-rigid	507.57	0.55	442.69	0.67	400.29	0.74	346.72	0.85
Pinned	175.12	1.43	167.48	1.49	165.85	1.54	164.12	1.64

5. Conclusions and recommendations

This study investigates the seismic behavior of 4, 6, and 8-story steel frames resting on elastic foundations using the non-linear pushover method. Performance levels were determined by drawing earthquake demand curves and capacity curves for each frame. Beam-column joints were considered in three different ways: rigid, semi-rigid, and pinned. The subsoil on which frames rest is represented by the Pasternak model. The results of the study are given below.

- It is observed that the horizontal displacements of the frames increase and, therefore, the horizontal load-carrying capacity of the frames decreases as the rotational stiffness of the beam-column joints decreases for all support cases.
- It is observed that base shear forces are larger as compared to fixed-based frames for all subsoil types. Contrary to expectations, the results for the assumption of a fixed base were approached as the subsoil softened. In the models with a fixed base, it is seen that the frames collapse at the column-foundation junction. However, The flexibility of the subsoil decreases the plastic rotations at the column-foundation joint.
- The results indicated that the subsoil flexibility can significantly change the response of the system, and neglecting soil-structure interaction may lead to an erroneous estimation of the seismic performance of the frame structures, especially those with flexible support.

Conflict of interests

The author(s) declared no potential conflicts of interest with respect to the research, authorship, and/or publication of this article.

Funding

This research received no external funding.

Data availability statement

No new data were created or analyzed in this study.

References

[1] Özer E (2015) Depreme dayanıklı çelik bina tasarımının temel ilkeleri ve yeni türk deprem yönetmeliği. 6. Çelik Yapılar Sempozyumu. Kongre Sempozyum Bildiriler Kitabı. Eskişehir, Türkiye (in Turkish).

[2] Krawinkler H, Seneviratna GDPK (1998) Pros and cons of a pushover analysis of seismic performance evaluation. Engineering Structure 20(4-6):452–464.

[3] Chopra AK, Goel RK (2004) A modal pushover analysis procedure to estimate seismic demands for unsymmetric-plan buildings. Earthquake Engineering and Structural Dynamics 33(8):903–927.

[4] Chintanapakdee C, Chopra AK (2003) Evaluation of modal pushover analysis using generic frames. Earthquake Engineering and Structural Dynamics 32(3):417–442.

[5] Kuran F, Bayülke N, Kocaman C (2003) 1502 Tipi afet konutunun nonlineer statik itme analizi ve deprem hasarının karşılaştırılması. Beşinci Ulusal Deprem Mühendisliği Konferansı. İstanbul, Türkiye (in Turkish).

[6] Edgar TH, Sordo E (2017) Structural behaviour of lattice transmission towers subjected to wind load. Structure and Infrastructure Engineering 13(11):1462–1475.

[7] Moghaddam H, Hajirasouliha I (2006) An investigation on the accuracy of pushover analysis for estimating the seismic deformation of braced steel frames. Journal of Constructional Steel Research 62(4):343–351.

[8] Kaley P, Baig MA (2017) Pushover analysis of steel framed building. Journal of Civil Engineering and Environmental Technology 4(3):301–306.

[9] Kalibhat MG, Kamath K, Prasad SK, Pai RR (2014) Seismic performance of concentric braced steel frames from pushover analysis. IOSR Journal of Mechanical and Civil Engineering pp:67–73.
[10] Mirjalili MR, Rofooei FR (2017) The modified dynamic-based pushover analysis of steel moment resisting frames. The Structural Design of Tall and Special Buildings 26:12.
[11] Computer and Structures Inc (2000) SAP2000 Structural Analysis and Design. Berkeley, CA, USA.
[12] ATC-40: Applied Technology Council (1996) Seismic Evaluation and Retrofit of Concrete Buildings. State of California.
[13] FEMA 356: Federal Emergency Management Agency (2004) Prestandart and Commentary for the Seismic Rehabilitation of Buildings. Washington, D.C.
[14] Tahaoğlu A (2017) Pasternak Türü Zemine Oturan Kirişlerin Zeminden Ayrılma Probleminin SAP2000 Yazılımı ile Çözümü. Yüksek Lisans Tezi, İstanbul Teknik Üniversitesi (in Turkish).